buildings

MDPI

Article

Infill Walls Effect on the Structural Performance of a RC Buildings Frame: A Study Based on Wall Modeling by Strut Element

Mehrzad Mohabbi

Department of Civil Engineering, Faculty of Engineering, Bingöl University, Bingöl 12000, Türkiye; mmohabbi@bingol.edu.tr

Abstract

This study investigates the seismic performance and behavior factors of reinforced concrete (RC) frames, focusing on the significant influence of masonry infill walls. While standard design codes like ACI-318, CSA-A23.3, and TBDY-2018 provide framework provisions, the structural contribution of infill walls is often neglected, leading to potential discrepancies between design assumptions and actual seismic response. The research employs a dual analytical approach, Nonlinear Static Pushover Analysis and Nonlinear Time History Analysis (NTHA), using ETABS 22 software. Four distinct structural configurations—Bare Frame (BF), Fully Infilled Frame (FIF), Partially Infilled Frame (PIF), and Soft Story Frame (SSF)—are evaluated to determine their overstrength, ductility reduction and response modification factors. The masonry infill walls are modeled using the equivalent diagonal strut method, accounting for their non-isotropic and brittle nature through parabolic stress–strain relationships. A core component of the study is the assessment of structural damage through a time-dependent Damage Index (DI), calculated by correlating displacement demands from NTHA with yield and ultimate displacements derived from idealized bilinear capacity curves. The findings highlight how the configuration of infill walls—specifically vertical and plan irregularities—modifies lateral stiffness, natural periods, and failure modes. The study concludes that accounting for the interaction between the RC frame and infill walls is critical for accurate seismic assessment, as these elements can transition failure mechanisms from ductile to brittle modes.

Keywords: reinforced concrete; infill walls; behavior factor; pushover analysis; damage Index; seismic performance; equivalent strut method

Check for updates

Academic Editors: Tadeh Zirakian and Salvatore Verre

Received: 24 February 2026
Revised: 23 March 2026
Accepted: 31 March 2026
Published: 3 April 2026

Copyright: © 2026 by the author. Licensee MDPI, Basel, Switzerland. This article is an open access article distributed under the terms and conditions of the Creative Commons Attribution (CC BY) license.

1. Introduction

Reinforced concrete (RC) design codes, such as ACI-318, CSA-A23.3 [1–3], establish specific provisions for the control and design of structures. In the seismic design of RC structures, engineers reduce the applied seismic forces based on the specific structural details employed. This reduction in elastic seismic force is achieved through a coefficient known as the behavior factor *R*. In RC structures, the behavior factor depends on several parameters, including the ductility factor, overstrength factor, redundancy factor, and damping factor. Among these, the ductility and overstrength factors play a fundamental role in determining the behavior factor of the structure. Research indicates that the axial force exerted on an RC member significantly influences its load–displacement curve and failure mode. Furthermore, high axial loads tend to shift the failure mechanism of RC members toward a brittle failure mode.

In a recent comprehensive study, Shaise K. John [4] and colleagues investigated the seismic performance of reinforced concrete (RC) structures, specifically focusing on substandard or earthquake-damaged components. Conducted within a laboratory environment in India, the research utilized half-scale square RC column specimens designed to represent real-world seismic vulnerabilities. To address these weaknesses, the authors proposed an innovative and sustainable Fabric-Reinforced Cementitious Matrix (FRCM) system, which substitutes traditional binders with a high-performance, fly ash-slag-based geopolymer mortar. The experimental phase subjected these specimens to constant axial loads and lateral cyclic forces to simulate rigorous seismic demands. In parallel, the study employed advanced Finite Element Modeling (FEM), utilizing the Concrete Damaged Plasticity (CDP) framework and a Traction-Separation Approach (TSA), to accurately predict stress distribution and bond-slip behavior. The results successfully demonstrated that strategic FRCM configurations—particularly those incorporating additional confinement in the plastic hinge regions—yielded a substantial increase in ductility, stiffness, and energy dissipation, effectively validating the system as a robust solution for the seismic retrofitting of aging or damaged infrastructure.

In a sophisticated comparative study, Francesco Fabbrocino [5] and his colleagues conducted a rigorous seismic assessment of Villa Vannucchi, a monumental historic structure in Italy. The research evaluates the efficacy of the Equivalent Frame Model (EFM), implemented via 3Muri software, by benchmarking it against an advanced Block-Based Method (BBM) utilizing Computational Limit Analysis (CLA). While the EFM approach proved to be a practical tool for capturing global 3D behavior—identifying a seismic risk coefficient of 0.508—it exhibited limitations in modeling the real-world impact of retrofitting interventions like steel tie-rods. Through "tilting tests" within the CLA framework, the authors demonstrated that tie-rods effectively redistribute forces, shifting the collapse mechanism from the upper floors to the foundation and enhancing global shear capacity. Ultimately, the study advocates for integrating limit analysis with standard codes to ensure more accurate and sustainable strategies for preserving architectural heritage.

1.1. Behavior Factor (Response Modification Factor)

Generally, the behavior factor of structures is expressed as a function of various parameters. These parameters include strength, ductility, damping, and structural redundancy, which can be calculated according to Equation (1):

$$R = R_s R_\mu R_{\tilde{\xi}} R_R \tag{1}$$

In the above equation:

- R_s is the overstrength factor,
- R_μ is the ductility reduction factor,
- $R_{\tilde{\xi}}$ is the damping factor,
- R_R is the redundancy factor of the structure.

The value of R_s is determined based on the yield strength and the strength corresponding to the formation of the first plastic hinge in the structure, according to Equation (2) (see Figure 1).

$$R_s = \frac{V_y}{V_s} \tag{2}$$

Extensive research has been conducted to calculate the ductility reduction factor. By providing analytical relationships based on a Single-Degree-of-Freedom (SDOF) system, researchers have determined the ductility factor of structures relative to their ductility and natural period. Notable studies include those by Newmark and Hall [6], Krawinkler and

Nassar [7], and Vidic et al. [8]. In this study, the relationship proposed by Newmark and Hall [6] is utilized to calculate the response modification factor, which is defined as follows in Equation (3):

$$R_\mu = 1 \quad T < 0.125\ \text{s}$$
$$R_\mu = \sqrt{2\mu - 1} \quad 0.125 < T < 0.5\ \text{s} \tag{3}$$
$$R_\mu = \mu \quad T > 5\ \text{s}$$

The value of the ductility reduction factor is significantly influenced by the structural ductility (μ), which is obtained by idealizing the structural capacity curve into a bilinear form and applying Equation (4). According to the above relationship, the amount of structural ductility depends on the ultimate displacement of the structure (Δ_u) and the yield displacement of the structure (Δ_y) (Figure 1).

$$\mu = \frac{\Delta_u}{\Delta_y} \tag{4}$$

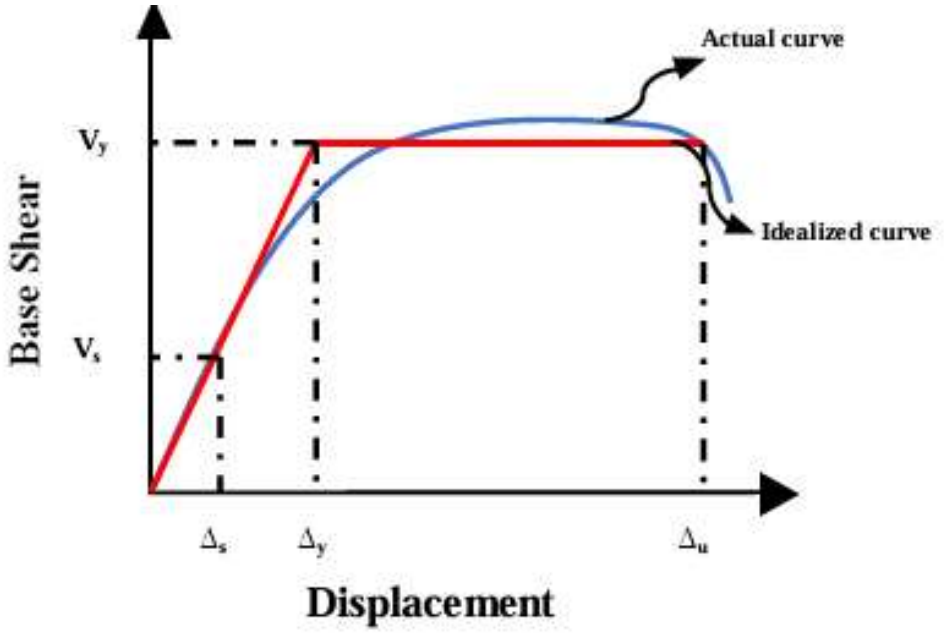

Figure 1. Base shear–roof displacement curve and bilinearization.

1.2. Infill Walls

In buildings, frames are commonly filled with masonry (brick) infill walls. The inclusion of these walls within a frame significantly alters its mechanical properties. These infill walls contribute to a substantial increase in the lateral stiffness of the structural system [7,9–13]. Furthermore, they modify the dynamic characteristics of the structure. Consequently, this causes the seismic behavior of the building to change due to the presence of these infill walls. It is noteworthy that the effects of infill walls are typically neglected in standard structural calculations and designs.

In the present study, the impact of infill walls on inter-story drift, story shear, and structural damage indices is investigated. Given the widespread use of brick infill walls in conventional buildings, studying their effect on structural behavior during earthquakes is a highly practical and significant topic. The combined system of the frame and the infill wall is referred to as a "composite frame". It can be stated that the design of composite frames is relatively complex.

Experiences from various earthquakes demonstrate that infill walls play a critical role in the seismic performance of structures. Although the presence of infill walls increases the overall stiffness of the structure, this change does not always yield positive results in terms of behavior. This modification in structural stiffness leads to significant alterations in performance. If the infill walls are placed asymmetrically in the building plan, it results in a shift in the center of stiffness, thereby increasing torsional forces. Additionally, an irregular distribution of infill walls along the height of the structure can cause significant discrepancies in the stiffness of different stories, leading to substantial changes in structural response.

The concept of an "equivalent strut" to represent brick infill walls was first proposed by Polyakov in 1960 [14]. Subsequently, researchers such as Holmes [15,16], Stafford Smith, and Mainstone [17,18] proposed various methods for determining the properties of the equivalent diagonal strut. In 1976, Klingner and Bertero [19] discovered that Mainstone's method offered superior accuracy based on experimental results. Numerous researchers have conducted studies on the modeling of infill walls, frequently employing Finite Element Method (FEM) analysis. Nonlinear analysis is commonly utilized to extract the properties of the equivalent diagonal strut for elastic modeling of infill walls based on a target displacement. Performing nonlinear analysis is an appropriate method to investigate the effects of infill walls on structures during seismic events. Since the "composite frame" system consists of two elements with distinct properties—the frame itself and the masonry infill wall—various assumptions must be integrated into the structural modeling. In the conventional design of structures, infill wall stiffness is usually not modeled precisely due to the heterogeneous, non-isotropic, and brittle nature of masonry materials. To ensure monolithic behavior between the frame and the infill wall, shear connectors are often used at the column–infill interface; if these connectors are absent, the structural response will differ significantly. A prevalent method for modeling infill walls is the use of an equivalent diagonal strut [15].

The stress–strain relationship of masonry materials in compression, as shown in Figure 2, is typically assumed to be parabolic up to the maximum stress $f\prime_m$. Subsequently, as strain increases, the stress decreases linearly before remaining constant.

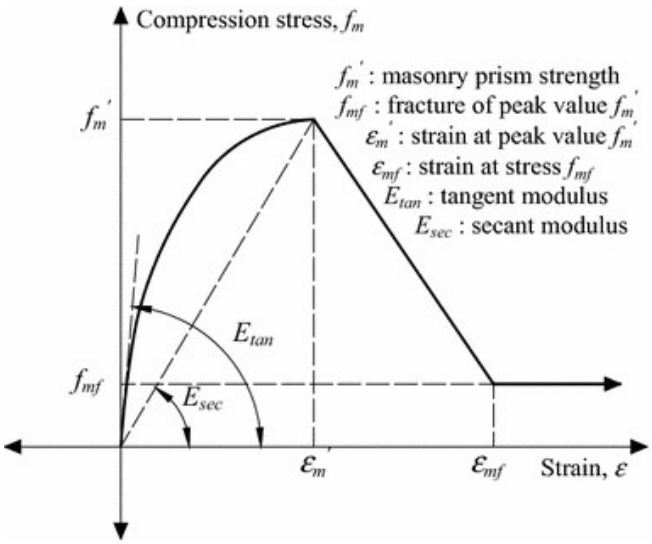

Figure 2. Stress–strain relationship of masonry materials in compression [20].

A highly effective method for modeling brick infill walls is the application of the equivalent strut. As seen in Figure 3, the underlying assumption is that these struts act only in compression.

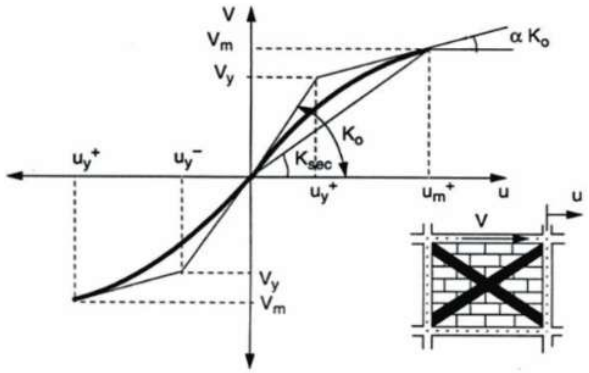

Figure 3. Constitutive model for masonry [21].

2. Materials and Methodology

2.1. Materials

For the structural system, C30 grade concrete and S420 reinforcing steel were utilized, with a 'high ductility' level adopted to comprehensively observe the effects of structural redundancy and energy dissipation on the overall behavior. The material constitutive models were defined in accordance with FEMA criteria.Specifically, the Mander confined concrete model was employed to accurately capture the strength and stiffness enhancement provided by transverse reinforcement. For the longitudinal reinforcement steel, a nonlinear simplified stress–strain relationship was implemented to represent post-yield performance.

Regarding the masonry infill, the equivalent diagonal struts were modeled to carry exclusively compressive forces, assuming zero tensile capacity in line with the physical nature of masonry–frame interaction. While the initial wall model followed a linear approximation for the strut properties provided in Table 1, the integration of these components into the nonlinear analysis framework allows for a representative simulation of the global structural response. This modeling approach ensures that the dominant role of infill walls in providing lateral stiffness is accurately reflected while maintaining computational efficiency.

Table 1. Column, beam, and strut cross-sections used in the models.

Sections	Dimensions (mm)	Reinforcement Pattern	Reinforcement Diameter (mm)	Clear Concrete Cover (mm)
Column	600 × 600	5 × 5	25	40
Beam	450 × 300	3 in top-3 in bottum	25	40
Strut	500 × 200	Without reinforcement	-	40

2.1.1. Selection of Ground Motion Records and Analytical Methodology

To comprehensively evaluate the seismic performance of the computational model and the structural influence of infill walls, the ground motion suite was selected to include three earthquake records with distinctly different seismological characteristics. This diversified selection subjects the proposed model to a rigorous "stress test" across varying energy levels, fault distances, and soil conditions, thereby enhancing the reliability and generalizability of the findings.

The selected suite includes the 1940 El Centro record (Figure 4) (Imperial Valley), a fundamental benchmark in seismic research [22] known for its broad frequency content. To bridge the gap between historical benchmarks and contemporary regional seismic demands, the record was re-scaled to reflect the high-intensity characteristics observed

at the Nurdağı (Fevzipaşa) station during the 2023 Kahramanmaraş event. Additionally, the Hollister station record from the 1989 Loma Prieta earthquake was incorporated to represent moderate acceleration levels on alluvial soil, while the Newhall station record from the 1994 Northridge earthquake was selected to capture high-acceleration near-fault effects. For all analyses, the first 30 s of these time-history recordswere utilized.

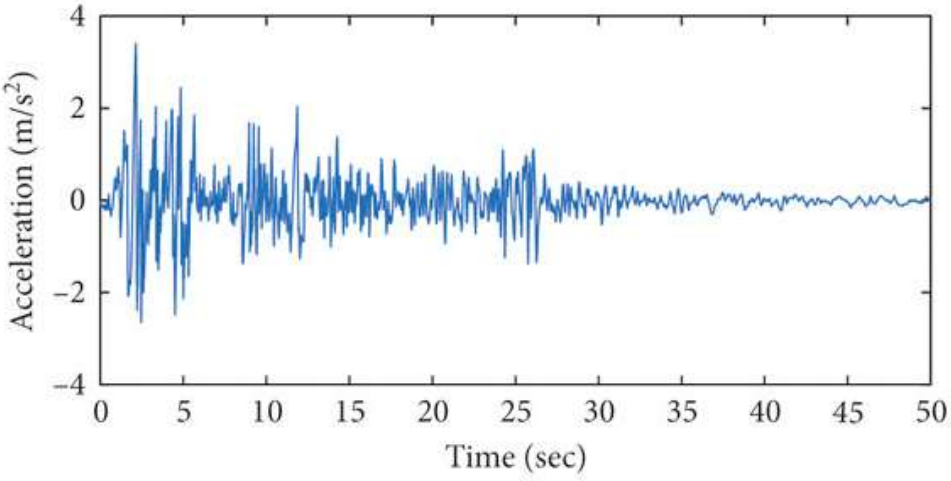

Figure 4. El Centro (1940) earthquake N-S component of ground motion acceleration time history.

2.1.2. The Cross-Sectional Details of the Columns, Beams and Strut Employed in the Nonlinear Analysis, Together with the Constitutive Material Properties of the Concrete, Reinforcing Steel, and Strut, Are Provided in Figure 5 and Table 1. Furthermore, the Intensities of the Additional Dead and Live Loads Applied to the Slabs and Beams Are Summarized in Table 2

Member dimensions, structural spans, and loading conditions are detailed in the subsequent tables. While the BF model represents the open frame, the distribution of infill walls varies across the other configurations: the FIF model incorporates walls in all stories, the SSF model contains walls only in the upper story, and the PIF model features walls solely in the lower story. Furthermore, the sectional data and masonry material properties for the equivalent strut models were defined based on FEMA criteria and are illustrated in Figure 5 and Table 1.

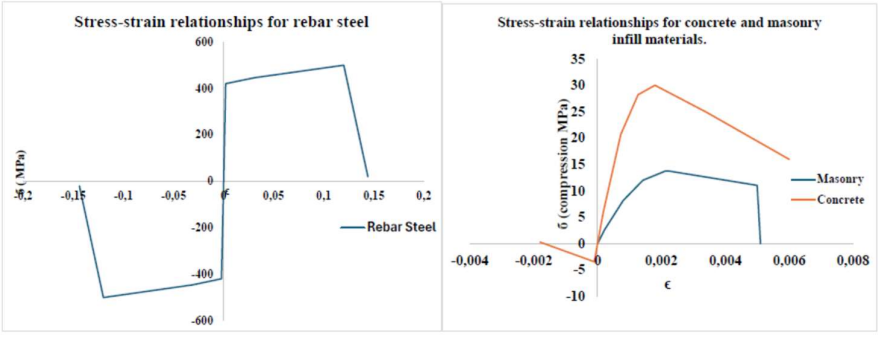

Figure 5. Stress–strain properties of the concrete, reinforcing steel, and strut.

Table 2. Additional dead and live load intensities for slabs and beams.

Loading	External Wall Loads	Slabs Load
Dead Load	5.884 1.471 kN/m	1.471 kN/m^2
Live Load	-	2.452 kN/m^2

The structural system of the building is characterized by a symmetrical and simplified geometry, featuring a single span in both principal orthogonal directions (X and Y). The structure consists of two stories, each with a consistent floor height of 3.5 m. Figure 6a.

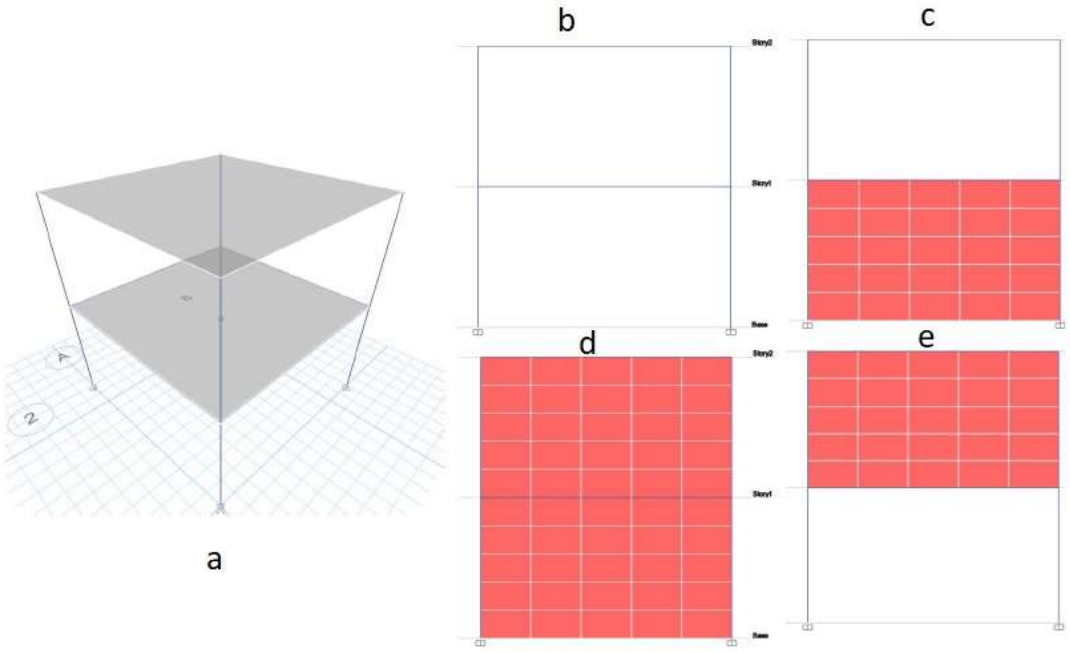

Figure 6. (**a**) 3D isometric view of the BF model; (**b**) front external wall view of the BF model; (**c**) front external wall view of the PIF model; (**d**) front external wall view of the FIF model; and (**e**) front external wall view of the SSF model.

2.2. Seismic Performance Analysis and Investigation of Infill Wall Effects

This study aims to determine the seismic performance parameters of two-story reinforced concrete (RC) frames with a constant height. Within the scope of the research, the effects of the presence and configuration of infill walls on the structural Damage Index (DI) were investigated using four different structural models:

- Model 1: Bare Frame (BF);
- Model 2: Fully Infilled Frame (FIF);
- Model 3: Partially Infilled Frame (PIF);
- Model 4: Soft Story Frame (SSF).

The structural design and seismic assessment were conducted in accordance with the principles of the 2018 Turkish Building Earthquake Code (TBDY).

Numerical analyses were performed using ETABS 22 software. Two fundamental methods were employed to determine structural performance:

Nonlinear Static Pushover Analysis

Conducted in compliance with FEMA-356 [12] standards, this analysis was used to obtain capacity curves, which were then idealized to calculate seismic parameters. The strength reduction factor due to ductility (R_μ) is determined based on the relationship between the natural period (T) and the characteristic period (T_B). Furthermore, the total response modification factor R is derived from the product of R_μ and the overstrength factor (Ω), where Ω is defined as the ratio of the yield shear force (V_y) to design the shear force (V_d).

If $T \geq T_B$ *then* $R_\mu = \mu$
If $T < T_B$ *then* $R_\mu = 1 + (\mu - 1)\frac{T}{T_B}$

As previously noted, while standard literature suggests that overstrength factors typically range between 1.5 and 2.5, the 2018 Turkish Building Earthquake Code (2018) [23] prescribes a higher range of 2.0 to 3.0 for such structural systems.

$$R \approx R_{\mu} \times \Omega$$

The findings obtained based on TBDY-2018 guidelines are provided in the Section 3, where a detailed discussion of these parameters is conducted.

Nonlinear Time History Analysis (NTHA): This method was utilized to measure the dynamic responses of the structures under seismic acceleration loads. Consequently, time-dependent Damage Index (DI) graphs were generated based on the analysis results.

2.3. Damage Index (DI) Calculations and Applied Methodology

In the first step, a control point must be selected, and based on this point, both nonlinear time-history analysis and nonlinear static (pushover) analysis should be performed. Subsequently, in order to utilize the results within the ETABS 22 software package, the outcomes of the pushover and time-history analyses must be extracted, and their corresponding response graphs should be generated [24].

One of the most critical aspects of this procedure is the determination of the yield displacement and the collapse (ultimate) displacement. To identify these displacement thresholds, various approaches have been proposed in the literature. The yield displacement can be determined using three commonly adopted methods:

- Idealized bilinear approximation method,
- Identification of the first significant stiffness degradation,
- Occurrence of the first widespread plastic hinge formation.

Similarly, the collapse displacement can be defined using the following three criteria:

- A reduction of 20% or more in the base shear capacity,
- Reaching the Collapse Prevention (CP) plastic hinge performance level,
- The displacement at which the nonlinear analysis terminates.

After completing these analyses and obtaining the required parameters from the pushover curve, the nonlinear time-history analysis is carried out, and the Damage Index (DI) is calculated. The nonlinear dynamic analysis yields a time-history displacement response, which is then used to compute the time-dependent Damage Index according to the following expression:

$$DI_{(t)} = \begin{cases} 0, & \Delta(t) \leq \Delta_y \\ \frac{\Delta(t)-\Delta_y}{\Delta_u-\Delta_y}, & \Delta_y \leq \Delta(t) < \Delta_u \\ 1, & \Delta(t) \geq \Delta_u \end{cases}$$

where $\Delta(t)$ is the displacement demand at time t, Δ_y is the yield displacement, and Δ_u is the collapse displacement.

Once the time history of $DI(t)$ is obtained, the maximum absolute value, denoted as DI_{max}, is adopted as the global damage index of the structural system.

3. Results and Discussion

3.1. Pushover Analysis Results and Discussion

The parameters obtained from the analyses, such as the overstrength factor, ductility factor, and structural behavior factor, are presented comparatively in Figure 7. It was observed that the presence of infill walls significantly alters the stiffness and energy dissipation capacity of the system. In particular, the SSF configuration induced a soft-story

irregularity that adversely influenced the structural behavior and deformation characteristics. All obtained data are detailed in the table and graphics.

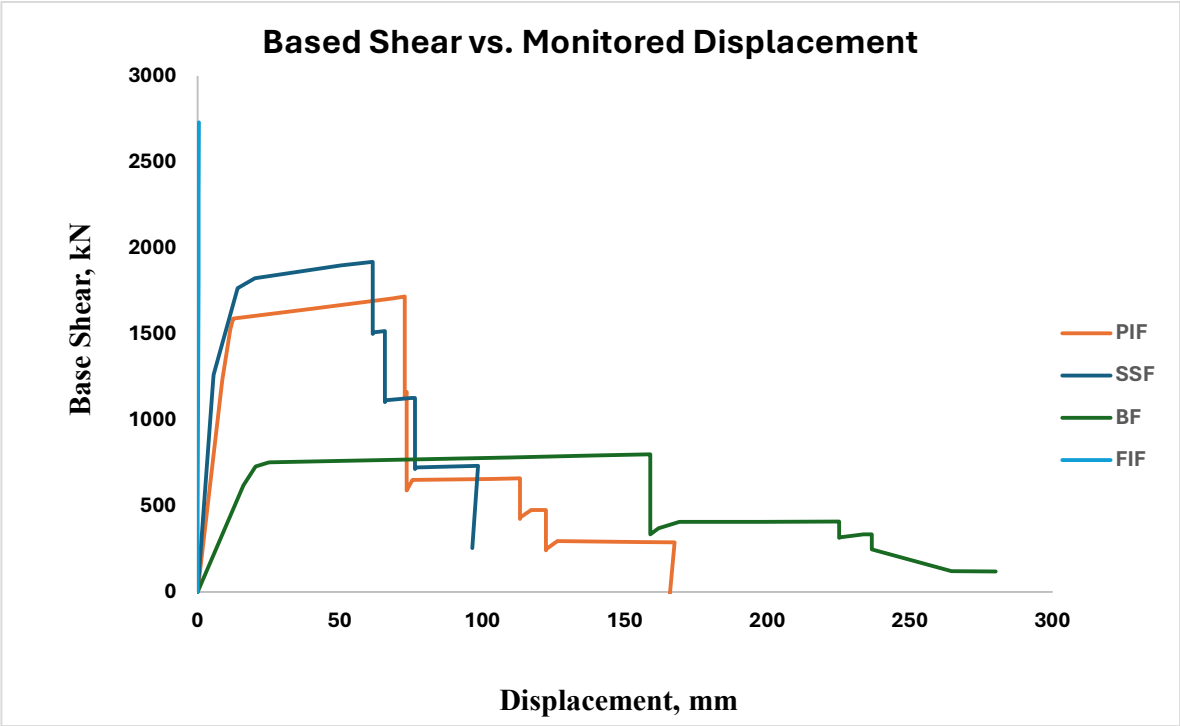

Figure 7. Based shear vs. monitored displacement in models.

In the models, the safety and adequacy of the design are confirmed by this result, assuming that R = 8 (high ductile reinforced concrete frames) was selected from the Turkish code during the initial design phase. The calculation of the response modification factor (R) requires the determination of the design shear force. In this study, the DD2 ground motion level for the Mustafa Gündoğdu neighborhood in Bingöl city center was selected for this procedure.

Both the pushover analysis parameters and the seismic demand variables were meticulously tailored to reflect the specific site conditions and regional seismic requirements of Bingöl. Following the static pushover procedure, the structural response data derived for the DD-2 hazard level—consistent with Bingöl's local demand spectrum—were consolidated into a comprehensive table (Table 3a,b).

1. Ductility and Displacement Capacity

The pushover analysis results indicate that the ductility ratios for the Soft Story Frame (SSF) and Bare Frame (BF) models are 6.98 and 13.76, respectively. A comparative evaluation reveals a significant deficiency in the ductility of the SSF system. The reduction in displacement capacity from 280 mm to 90 mm is a direct consequence of the soft-story irregularity. These findings demonstrate that the SSF configuration fails to meet favorable seismic performance criteria.

2. Shear Capacity and Failure Mechanism

The elevated base shear capacity observed in the SSF model during pushover analysis is inherently misleading. Although the peak strength appears high, the ultimate displacement capacity du = 98.38 mm is approximately 65% lower than that of the bare frame du = 280 mm. This trend signifies a severe restriction in the structure's energy dissipation capacity. The concentration of plastic deformations within a single floor suggests that the

building loses stability prematurely, leading to a high risk of sudden and brittle collapse in the lower story, a highly undesirable failure mode in seismic design.

Table 3. (**a**) Pushover analysis parameters and the seismic demand variables. (**b**) Dimensionless parameters derived from pushover analysis and seismic demand variables.

(**a**)										
Model Type	**K_e (KN/mm)**		**V_y (kN)**		**d_y (mm)**		**V_{max} (kN)**		**d_u (mm)**	
	Raw Data	TBDY2018	Raw Data	TBDY2018	Raw Data	TBDY2018	Raw Data	TBDY2018	Raw Data	TBDY2018
(BF)	35.85	33.33	729.63	750	20.35	22.50	799.29	750	280.00	158.85
(PIF)	133.65	225.90	1526.23	1620	11.42	7.17	1716.88	1620	167.33	72.65
(SSF)	125.30	225.80	1766.78	1850	14.10	8.19	1918.13	1850	98.38	61.52
(FIF)	5687.35	5687.35	2729.93	2729.9	0.48	0.48	2729.93	2729.9	0.48	0.48
(**b**)										
Model Type	**$M = \frac{d_u}{d_y}$**		**α**		**Ω**		**R_μ**		**R**	
	Raw Data	TBDY2018	Raw Data	TBDY2018	Raw Data	TBDY2018	Raw Data	TBDY2018	Raw Data	TBDY2018
(BF)	13.76	7.06	0.30	0	2.02	2.08	5.15	3.62	10.40	7.53
(PIF)	14.65	10.13	0.023	0	4.23	4.49	5.32	4.39	22.50	19.71
(SSF)	6.98	7.51	0.014	0	4.89	5.12	3.60	3.74	17.62	19.15
(FIF)	1	1	0	0	7.56	7.56	1	1	7.56	7.56

3. Regulatory Compliance and Safety Margins

The TBDY 2018 (Turkish Building Earthquake Code) guidelines provide conservative estimates regarding the detrimental effects of infill walls on ductility. The fact that the code-predicted values for PIF (Partially Infill Frame) and SSF models remain lower than the experimental/analytical data is a deliberate approach that enhances the safety margin in structural design.

4. Influence of Infill Walls on Stiffness

Infill walls significantly increase the in-plane stiffness of the reinforced concrete frame. The extreme stiffness surge observed in the Fully Infill Frame (FIF) model suggests that the walls act as "equivalent diagonal struts," allowing the system to emulate the structural rigidity of a shear wall.

5. Dynamic Characteristics and Period Dominance

The presence of infill walls in even a single story (as seen in PIF or SSF models) results in a 270% increase in global initial stiffness compared to the BF model. This confirms that infill walls dominate the dynamic characteristics of the structural system, specifically affecting its natural period and frequency.

6. Discrepancy Between Raw Data and TBDY 2018

The discrepancy where TBDY 2018 values for PIF and SSF models are higher than "Raw Data" values stems from the code's tendency to predict a higher initial stiffness. By assuming a higher stiffness, the design process adopts a shorter natural period, which subjects the structure to higher calculated seismic forces. This approach serves as a safety buffer during the design phase.

7. Comparative Stiffness Analysis

The stiffness of the SSF model (125.30) is slightly lower than that of the PIF model (133.65). The absence of infill walls in the bottom story increases the system's propensity for lateral deformation, which accounts for this marginal decrease in initial stiffness.

8. The "Seismic Magnet" Effect and Optimal Performance

The transition from a "flexible frame" to a "rigid block" behavior, induced by infill walls, leads to an increase in base shear forces. While a lower base shear in the BF model is an advantage due to flexibility (reducing the load on foundations and members), the FIF model sees this value spike to 2729 kN. While high strength is generally positive, it attracts seismic loads like a "magnet," which becomes hazardous if ductility is low.

Analysis shows that while the FIF model maximizes strength, it risks brittle failure by eliminating ductility. Conversely, the SSF model creates a soft story irregularity, undermining the capacity of the bare frame. The PIF model emerges as the most balanced solution, offering both reasonable strength enhancement and superior seismic stability compared to the SSF. The high ductility value (R = 22.50) observed in the PIF model highlights the significant energy dissipation potential provided by the composite action between the frame and infill walls

3.2. Nonlinear Time-History Analysis Results and Discussion

To ensure computational efficiency and prevent potential convergence issues during the nonlinear simulations, modified time-history functions with a discretized time step of 0.1 s were utilized. In this study, the seismic input was expanded to include three distinct ground motion records to validate the structural response's independence from seismic characteristics and to confirm the damping efficacy of the infill walls. These records encompass the 1940 El Centro earthquake as a historical benchmark, the 1994 Northridge earthquake to represent near-fault effects, and the 1989 Loma Prieta event to reflect moderate-intensity ground motion.

The seismic inputs were precisely scaled to match the high-intensity acceleration characteristics observed at the Nurdağı (Fevzipaşa) Station during the 2023 Kahramanmaraş earthquake sequence. These scaled acceleration records are visually detailed in Figure 8a–c. The findings indicate that across these three diverse seismic scenarios with varying spectral contents and energy levels, the structural behaviors—specifically story drifts and damage indices—exhibited a remarkably consistent and parallel trend.

Notably, models incorporating infill walls (FIF and PIF) demonstrated a dramatic reduction in maximum displacements across all seismic records compared to the Bare Frame (BF) model. This correlation, maintained despite varying earthquake characteristics, validates the accuracy of the equivalent diagonal strut model and proves that the increased structural stiffness stabilizes the system regardless of the seismic input type. Furthermore, by evaluating the mean results, aleatory uncertainties inherent in individual records were minimized, providing a more robust and scientifically reliable foundation for the proposed design parameters.

Evaluation of Nonlinear Time History Analysis Results

The results of the nonlinear time-history analysis (NLTHA) demonstrate a high degree of correlation with the initial stiffness values obtained from the static pushover analysis, reinforcing the premise that displacement demands are inversely proportional to structural stiffness. A synergistic evaluation of the peak response data presented in Table 4, coupled with the Damage Index (DI) formulation, provides a quantitative roadmap of how infill wall configurations fundamentally transform structural performance.

The Bare Frame (BF) model consistently bore the highest seismic demand across all scenarios, peaking at 25.09 mm under the Northridge record. This response is directly attributable to its lower lateral stiffness and longer natural period, which increase its vulnerability to high-intensity ground motions. In stark contrast, the Fully Infilled Frame (FIF) model demonstrated exceptional energy mitigation, suppressing displacements to

below 0.1 mm (specifically 0.029 mm under El Centro). This confirms that the extreme stiffness provided by masonry infills leads to a quasi-rigid structural response, resulting in a near-zero damage margin (DI ≈ 0).

A comparative analysis of the partially infilled models offers critical insights into the "Soft Story" phenomenon and structural discontinuities. Under the El Centro record, the PIF configuration (2.46 mm) proved to be approximately 11.5% stiffer than the SSF model (2.78 mm). This trend of vulnerability in the SSF model—where the vacant first story is forced to undergo larger deformations to dissipate energy—was further corroborated by the Northridge and Loma Prieta scenarios, where displacements climbed to 4.70 mm and 6.03 mm, respectively. These findings numerically validate the structural risks caused by the upward shift in the center of rigidity, a classic hallmark of soft-story irregularity.

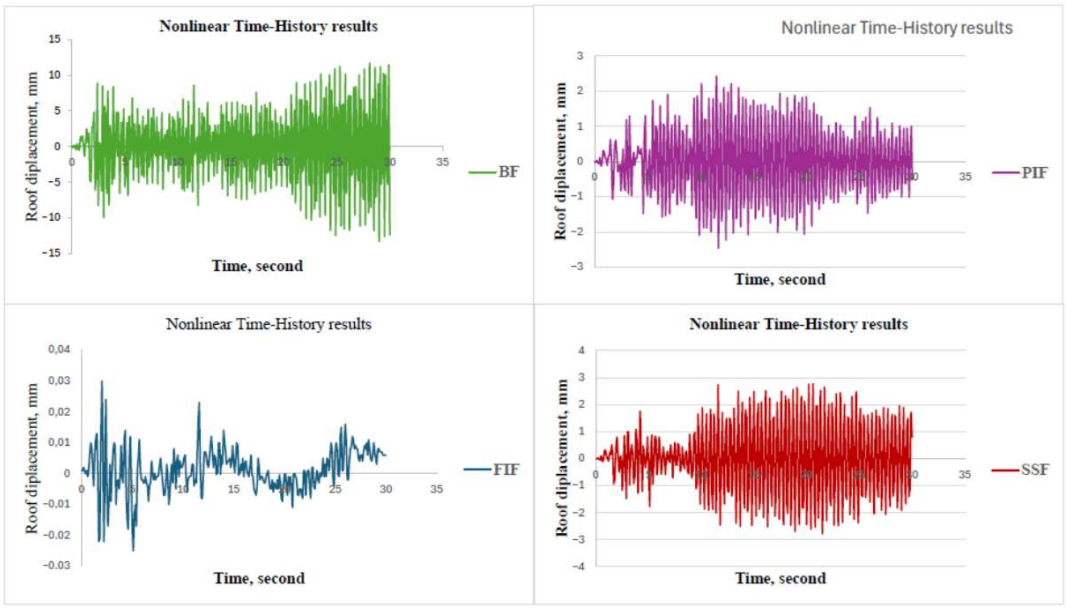

(**a**)

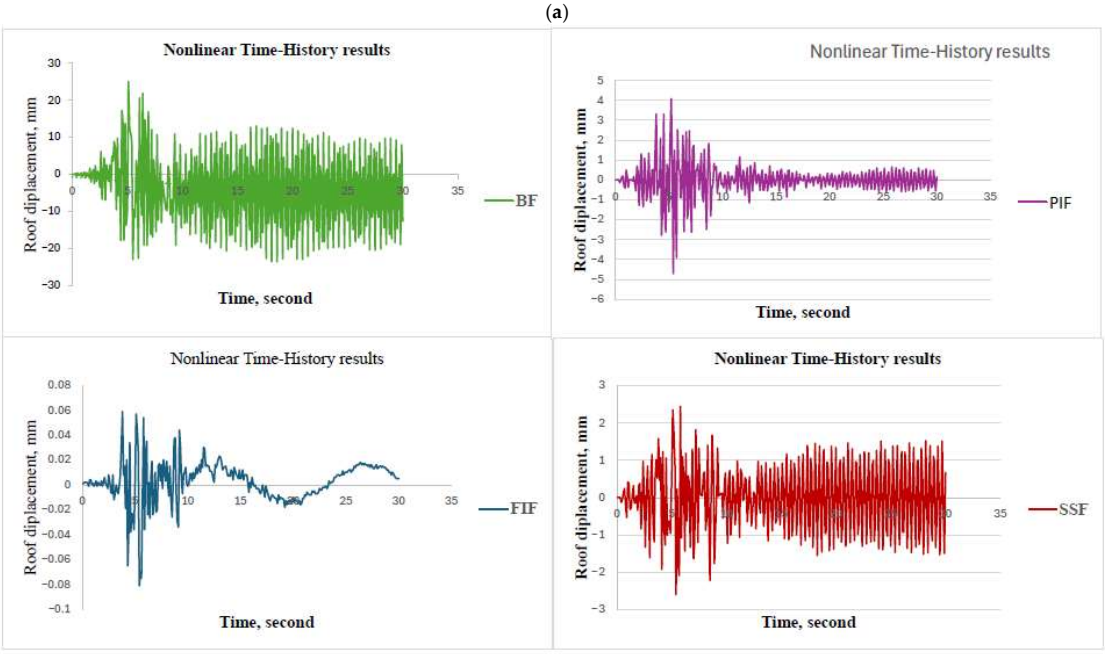

(**b**)

Figure 8. *Cont.*

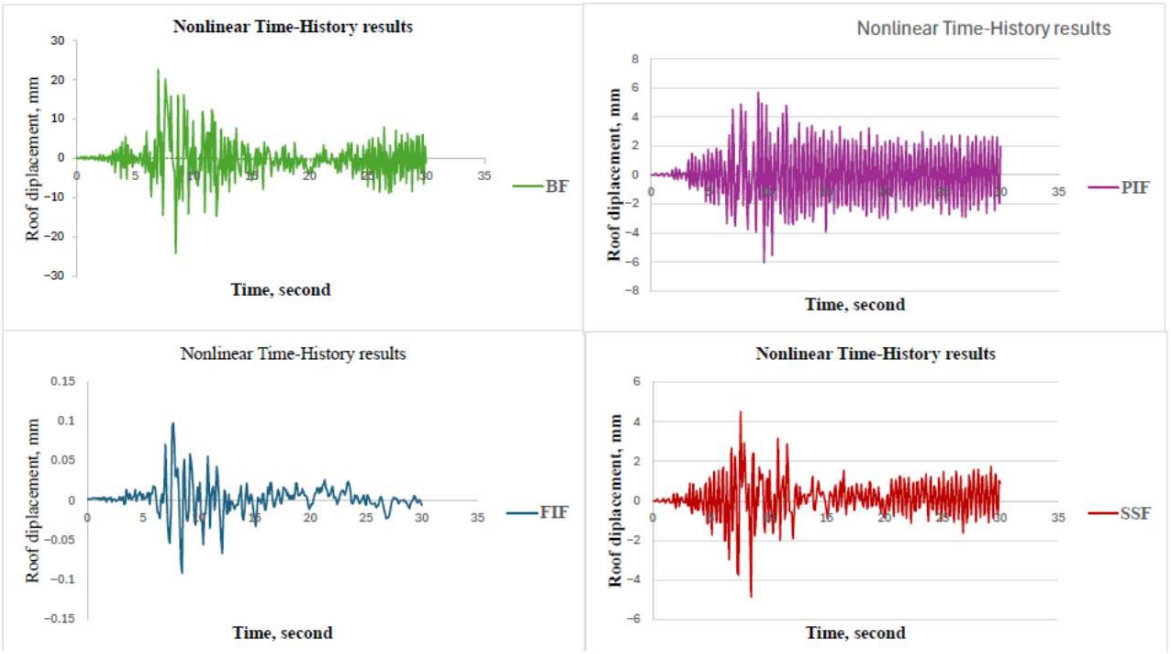

(**c**)

Figure 8. (**a**) Comparative Seismic Response of Model Types under the El Centro Earthquake Record. (**b**) Comparative seismic response of structural models under the 1994 Northridge (Newhall Station) earthquake record. (**c**) Comparative seismic response of structural models under the 1989 Loma Prieta (Hollister Station) earthquake record.

Table 4. Maximum lateral displacements (mm) of the four model configurations under El Centro, Northridge, and Loma Prieta records.

	The Maximum Displacement Under Ground Motion Record (mm)		
Description of Structural Models	**El Centro (1940)**	**Northridge (1994)**	**LOMA PRIETA (1989)**
BF	13.28	25.09	24.20
FIF	0.029	0.08	0.098
PIF	2.46	4.70	6.03
SSF	2.78	2.59	4.85

Despite these varying seismic demands and the diverse spectral contents of the three earthquake records, the peak DI values across all configurations remained remarkably low, ranging between 0.012 and 0.018. Since these values stay well below the 0.1 damage threshold, it is evident that the structural system retains a substantial reserve capacity, consistently operating within the 'Immediate Occupancy' performance level. This confirms that the maximum displacements DeltaΔ(t) do not approach the critical yield threshold Δy in any of the analyzed scenarios. Ultimately, these findings underscore that the strategic spatial distribution and structural continuity of masonry infills are not merely beneficial but paramount for ensuring stable seismic behavior and insulating the structure against significant degradation.

3.3. Seismic Damage Assessment and Interpretation

The seismic damage indices (DI) for all structural configurations were calculated as zero, indicating that the system response remained entirely within the elastic range under the prescribed seismic demand. In the infilled models (PIF, SSF, and FIF), the substantial increase in lateral stiffness effectively limited deformation demands to levels

below the threshold of plastic hinge formation. Although the Bare Frame (BF) model exhibited higher displacement demands, the structural capacities proved sufficient to withstand the excitation without incurring permanent damage. These results signify that the energy dissipation was primarily governed by the system's inherent damping rather than material degradation, ensuring the maintenance of full structural integrity across all examined scenarios.

4. Conclusions

This research presents a comprehensive evaluation of how masonry infill wall configurations dictate the seismic response of RC frames, integrating findings from nonlinear static pushover and time-history analyses (NLTHA) using three distinct ground motion records. The following key conclusions are drawn from the analytical results:

1. **Correlation of Analytical Methods:** The NLTHA results demonstrate a high degree of correlation with the initial stiffness values obtained from static pushover analysis. This synergy confirms that the structural response is fundamentally governed by the stiffness–displacement relationship, where displacement demands are inversely proportional to the system's lateral rigidity.
2. **Superiority of the PIF Configuration:** The Partially Infilled First-Story (PIF) model emerged as the most resilient configuration. It achieved a 270% increase in initial stiffness compared to the Bare Frame (BF) while maintaining a high behavior factor (R = 22.50). This balance ensures optimal energy dissipation and structural stability.
3. **Risks of the SSF (Soft-Story) Mechanism:** The SSF configuration serves as a critical cautionary case for structural irregularity. Despite its apparent strength, the SSF model exhibited an 11.5% increase in dynamic displacement compared to the PIF model and a 65% reduction in displacement capacity. This numerically validates that infilling only the upper stories triggers a "soft-story" mechanism, concentrating seismic energy and deformations at the ground level.
4. **Impact of Infill on Global Response:** The Fully Infilled Frame (FIF) demonstrated exceptional mitigation of seismic energy, suppressing displacements to below 0.1 mm (0.029 mm under El Centro). This transition to a quasi-rigid response results in a near-zero damage margin (DI $\approx$ 0), proving the insulation capacity of masonry against seismic degradation.
5. **Seismic Performance and Damage Thresholds:** Across three spectrally diverse seismic records (El Centro, Northridge, and Loma Prieta), the peak Damage Index (DI) values remained remarkably low, ranging between 0.012 and 0.018. Since these values stay well below the 0.1 threshold, the study confirms that the structure maintains a substantial reserve capacity and operates within the 'Immediate Occupancy' performance level.
6. **Robustness of the Modeling Approach:** The consistency of results across varying earthquake scenarios, ranging from near-fault effects (Northridge) to moderate intensity ground motions (Loma Prieta), validates the accuracy of the equivalent diagonal strut model. Utilizing mean results from spectrally diverse records minimized aleatory uncertainties, providing a reliable scientific basis for design.
7. **Design Recommendations and Code Alignment:** Comparison with the TBDY-2018 code highlights that conservative stiffness predictions are vital safety buffers. To achieve stable seismic performance, infill walls must be strategically placed to ensure structural continuity. The findings strongly advocate for the PIF strategy while emphasizing that the SSF configuration should be strictly avoided in high-seismic risk regions.

https://doi.org/10.3390/buildings16071423

The results clearly demonstrate that while infill walls significantly bolster lateral stiffness and shear capacity, their spatial arrangement is the most critical factor in ensuring structural resilience.

The PIF (First-Story Infilled) model emerged as the most effective configuration, striking an optimal balance between strength and ductility. By achieving a 270% increase in initial stiffness compared to the bare frame while maintaining a high behavior factor R = 22.50, the PIF model demonstrates a superior capacity for energy dissipation. In contrast, the SSF (Soft-Story) model serves as a cautionary example of structural irregularity. Despite its apparent high strength, the SSF model suffered a 65% reduction in displacement capacity and exhibited an 11.5% increase in dynamic displacement compared to the PIF model. This confirms that infilling only the upper stories creates a "soft-story" mechanism that concentrates damage at the ground level, leading to a high risk of premature collapse.

Furthermore, the comparison with TBDY 2018 reveals that the code's conservative stiffness predictions act as a necessary safety buffer, ensuring that structures are designed for higher seismic demands than raw analytical data might suggest. Ultimately, this study concludes that to achieve stable seismic performance, infill walls must be placed to ensure structural continuity. The findings strongly advocate for the PIF strategy for resilient design while emphasizing that the SSF configuration should be strictly avoided due to its localized deformation demands and lack of reliable ductility.

Limitations of the Research

While this study provides significant insights into how masonry infill configurations dictate the seismic response of RC frames, certain limitations must be acknowledged to provide a balanced context for the findings:

- **Structural Geometry and Scale:** The analytical investigations were confined to a symmetrical, two-story RC frame with a single span in both principal directions and a consistent floor height of 3.5 m. Consequently, the interaction between infill walls and the frame might exhibit different dynamic characteristics in high-rise structures or irregular buildings with multi-span configurations.
- **Material Variability:** The numerical models utilized specific material grades, namely C30 concrete and S420 reinforcing steel, to observe redundancy and energy dissipation. The influence of varying concrete strength classes or different masonry unit properties on the overall structural ductility and stiffness remains outside the scope of this particular evaluation.
- **Seismic Record Suite:** Although the study employed three distinct ground motion records—El Centro, Northridge, and Loma Prieta—scaled to match high-intensity regional characteristics, the results are inherently linked to these specific spectral contents. Utilizing a broader suite of earthquake data could further enhance the statistical generalizability of the seismic performance parameters.
- **Modeling Assumptions:** The masonry infills were represented using the equivalent diagonal strut method, which assumes that the struts act exclusively in compression with zero tensile capacity. While this approach effectively captures global structural behavior and stiffness, it does not explicitly account for local failure modes, such as out-of-plane expulsion or detailed shear-cracking patterns within the masonry panels.

Funding: This research received no external funding and the Article Processing Charge (APC) was funded by the author; the study was conducted independently without any public or private project support.

Data Availability Statement: The original contributions presented in the study are included in the article, further inquiries can be directed to the corresponding author.

Acknowledgments: Portions of this study were refined using AI-assisted technologies for language editing and academic translation to enhance the clarity of the technical analysis. The author reviewed and approved all generated content before submission.

Conflicts of Interest: The author declares no conflict of interest.

References

1. American Concrete Institute. *Building Code Requirements for Structural Concrete (ACI 318-08) and Commentary*; American Concrete Institute: Farmington Hills, MI, USA, 2008.
2. *CSA Standard A23.3-04*; Design of Concrete Structures. CSA Group: Toronto, ON, Canada, 2004.
3. Ghorbanirad, Y. Evaluation of Iranian Building Codes and Standards Provided for Steel and Concrete Structures in Industrial Buildings in the Case of Making a Contract Between Iran and Finland. Bachelor's Thesis, Tampere University of Applied Sciences, Tampere, Finland, 2018.
4. John, S.K.; Cascardi, A.; Verre, S.; Nadir, Y. RC-columns subjected to lateral cyclic force with different FRCM-strengthening schemes: Experimental and numerical investigation. *Bull. Earthq. Eng.* **2025**, *23*, 1561–1590. [CrossRef]
5. Fabbrocino, F.; Olivieri, C.; Luciano, R.; Vaiano, G.; Maddaloni, G.; Iannuzzo, A. Seismic performance of historic masonry buildings: A comparative analysis of equivalent frame and block-based methods. *Alex. Eng. J.* **2024**, *109*, 359–375. [CrossRef]
6. Newmark, N.M.; Hall, W.J. *Earthquake Spectra and Design*; Engineering Monographs on Earthquake Criteria; Earthquake Engineering Reach: Telangana, India, 1982.
7. Krawinkler, H.; Nassar, A.A. Seismic design based on ductility and cumulative damage demands and capacities. In *Nonlinear Seismic Analysis and Design of Reinforced Concrete Buildings*; CRC Press: Boca Raton, FL, USA, 1992; pp. 31–48.
8. Vidic, T. Procedure for determining consistent inelastic design spectra. *Nonlinear Seism. Anal. Des. Reinf. Concr. Build. Suppl. Proc. A Work. Held Bled* **1992**, *103*, 9–32.
9. Smith, B.S. Lateral stiffness of infilled frames. *J. Struct. Div.* **1962**, *88*, 183–199. [CrossRef]
10. Smith, B.S. Behavior of square infilled frames. *J. Struct. Div.* **1966**, *92*, 381–404. [CrossRef]
11. Smith, B.S. Model test results of vertical and horizontal loading of infilled frames. *J. Proc.* **1968**, *65*, 618–625.
12. Federal Emergency Management Agency (FEMA). *Prestandard and Commentary for the Seismic Rehabilitation of Buildings (FEMA 356)*; Federal Emergency Management Agency: Washington, DC, USA, 2000; Volume 7, p. 518.
13. Pokhrel, A.; Gautam, D.; Chaulagain, H. Effect of variation on infill masonry walls in the seismic performance of soft story RC building. *Aust. J. Struct. Eng.* **2019**, *20*, 1–9. [CrossRef]
14. Polyakov, S. On the interaction between masonry filler walls and enclosing frame when loaded in the plane of the wall. *Transl. Earthq. Eng.* **1960**, *2*, 36–42.
15. Holmes, M. Steel frames with brickwork and concrete infilling. *Proc. Inst. Civ. Eng.* **1961**, *19*, 473–478. [CrossRef]
16. Holmes, M. Combined loading on infilled frames. *Proc. Inst. Civ. Eng.* **1963**, *25*, 31–38. [CrossRef]
17. Mainstone, R.J. On the stiffness and strength of infilled frames. *Proc. Inst. Civ. Eng.* **1971**, *49*, 57. [CrossRef]
18. Mainstone, R.J. *Supplementary Note on the Stiffnesses and Strengths of Infilled Frames*; Building Research Establishment, Building Research Station: Watford, UK, 1974.
19. Klingner, R.E.; Bertero, V. *Infilled Frames in Earthquake-Resistant Construction*; University of California, Berkeley: Berkeley, CA, USA, 1977.
20. El Zareef, M.A.; El Madawy, M.E. Optimization of infill panel for seismic response of multi-story RC frame buildings utilizing multi criteria optimization technique. *Bull. Earthq. Eng.* **2018**, *16*, 4951–4970. [CrossRef]
21. Karami, F.; Izadpanah, M. Incremental inelastic dynamic damage analysis of MRRCFs infilled with masonry panels. *J. Build. Eng.* **2021**, *44*, 103282. [CrossRef]
22. Neumann, F. The analysis of the El Centro record of the Imperial Valley earthquake of May 18, 1940. *Eos Trans. Am. Geophys. Union* **1941**, *22*, 400. [CrossRef]
23. *TBDY-2018*; Turkish Building Earthquake Code. Disaster and Emergency Management Authority (AFAD): Ankara, Turkey, 2018.
24. Ghobarah, A.; Abou-Elfath, H.; Biddah, A. Response-based damage assessment of structures. *Earthq. Eng. Struct. Dyn.* **1999**, *28*, 79–104. [CrossRef]

Disclaimer/Publisher's Note: The statements, opinions and data contained in all publications are solely those of the individual author(s) and contributor(s) and not of MDPI and/or the editor(s). MDPI and/or the editor(s) disclaim responsibility for any injury to people or property resulting from any ideas, methods, instructions or products referred to in the content.